Desalination and Water Treatment
www.deswater.com

doi: 10.5004/dwt.2023.29926

308 (2023) 68–79
October

Investigation of the synergistic effect of the Fenton process on the paint industry wastewater treatment and optimization of independent process parameters

Ömer Apaydin*, Uğur Kurt, Fatih İlhan

Yildiz Technical University, Faculty of Civil Engineering, Department of Environmental Engineering, Davutpaşa Campus, 34220 Esenler, Istanbul, Turkey, Tel.: +90 2123835387; email: apaydin@yildiz.edu.tr (Ö. Apaydin), Tel.: +90-212-3835392; email: ukurt@yildiz.edu.tr (U. Kurt), Tel.: +90-212-3835396; email: filhan@yildiz.edu.tr (F. İlhan)

Received 26 April 2023; Accepted 28 August 2023

ABSTRACT

Paint industry wastewater is hard to treat due to its complex and changing structure. In the study, the Fenton oxidation process was used to treat this wastewater. The pH levels required for the Fenton process were obtained without any chemical addition other than Fenton's catalyst and oxidant. Reaction time, H_2O_2 concentration, and Fe^{2+} concentration were chosen as independent parameters for the experimental design employing Taguchi orthogonal arrays. These independent parameters were varied at four different levels to find out their effects on the removal efficiencies of the dependent parameters. Chemical oxygen demand (COD) and color were chosen as the dependent parameters. The removal efficiencies of COD and color were obtained at 69% and 98%, respectively. According to optimization studies, the degree of effect of H_2O_2 concentration, Fe^{2+} concentration, and reaction time on COD removal performance were obtained as 12.01%, 23.87%, and 21.67%, respectively. Moreover, the degree of effect on color removal performance of H_2O_2 concentration, Fe^{2+} concentration, and reaction time were obtained as 15.08%, 19.00%, and 22.42%, respectively. Furthermore, the results from this experimental optimization study show that the synergistic effect of Fenton oxidation on COD removal provides additional removal efficiency reaching 190% compared with H_2O_2's real oxidation potential.

Keywords: Fenton process; Optimization; Paint industry wastewater; Synergistic effect; Treatability

1. Introduction

Paint industry wastewater (PIWW) is industrial wastewater that requires many treatment processes because it contains organic and inorganic pollutants that can be difficult to remove [1]. PIWW may contain lots of contaminants such as chemical oxygen demand (COD), biochemical oxygen demand, suspended and dissolved solids, oil and grease, and heavy metals in extreme concentrations; for that reason, it may be necessary to use different treatment combinations for the removal of pollutants. Today, many methods such as physical–chemical [2], chemical–biological [3–5], coagulation–flocculation [6–8], coagulation–electrochemical [9–12], advanced oxidation [13–15], and membrane processes [16] are applied for the treatment of PIWW. Advanced oxidation processes (AOPs), which are one of the PIWW methods, can be classified under four main headings: chemical, photochemical, sonochemical, and electrochemical [1,17]. Some information about AOPs, which are still widely used in water and wastewater treatment studies today, is given in Fig. 1.

In this study, Fenton reagent, one of the methods given under the title of chemical AOPs, was applied. As is known, a combination of H_2O_2 and a homogeneous solution of iron ions is described as Fenton's reagent, and the application of Fenton's reagent in any process is called the Fenton

* Corresponding author.

process. The methods applied today regarding the Fenton processes are given in Fig. 2.

The basic parameters to be considered in PIWW treatment can be given as independent factors in the optimization process, and the pollutant removal efficiencies are determined depending on the optimized concentrations of these independent factors. As a result, it is essential to optimize independent factors to increase treatment efficiency. In addition, in classical optimization, all factors are optimized one by one while keeping the other factor levels constant. For this reason, the number of experimental studies and workload required in the classical optimization method can cause time losses [19]. It is well known that there are many statistical experimental design practices that are generally used, such as full or partial factorial designs, response surface methodology, and the Taguchi method [20–28]. The Taguchi method entails the planning of a trial using orthogonal arrays (OA) to permit free estimation of factors in a minimum number of experiments. This method involves transferring the formation obtained from experimental studies to a signal-to-noise (S/N) fraction. The Taguchi method has the ability to examine the factors that can affect any experimental study at a controlled or uncontrolled level and is a flexible experimental design and evaluation application formed by many design factors [29].

In the current study, treatability studies with the Fenton process were carried out on a sample taken from the wastewater equalization pool of a factory that produces paints and chemicals for the textile, plastic, metal, and paper industries. Some basic chemical and physical parameters of the PIWW are presented in Table 1.

As seen in Table 2, PIWW has highly loaded wastewater characteristics (COD > 6 g/m^3). That's why the Fenton process is suitable for the treatment of discharges loaded with dyes. In order to treat PIWW, the Fenton process was carried out using $FeSO_4 \cdot 7H_2O$ as the Fenton's catalyst in batch studies in the laboratory. The aim of the current study is to investigate the treatability of PIWW using the Taguchi method, determine which levels of independent variables have the highest pollutant removal efficiency, and optimize the removal rate of pollutants. Therefore, a working matrix was planned using the Taguchi method, a module on the Minitab 19 software (using L_{16} orthogonal arrays). Based on this planned matrix, batch studies were carried out.

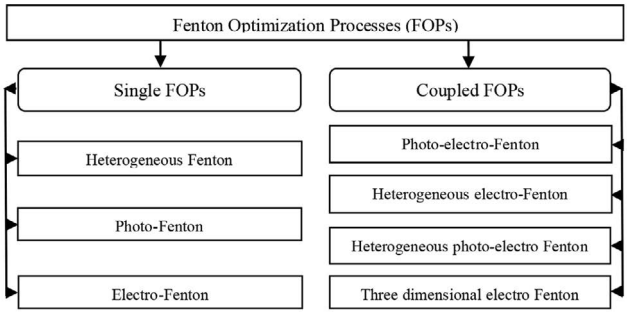

Fig. 2. Fenton processes.

Table 1
Characteristics of paint industry wastewater

Parameters	Values
pH (at 20°C)	5.5–5.9
Conductivity, mS/cm (at 20°C)	13.2–13.4
Chemical oxygen demand, g/L	6.2–6.6
Color, Pt-Co, unit	24,000–28,000

Table 2
Factors and their values corresponding to the levels to be studied in the Fenton experiments

Experimental factors	Experimental levels			
	1	2	3	4
A: H_2O_2, g/L	2.9	5.8	8.7	11.6
B: Fe^{2+}, g/L	0.14	0.29	0.44	0.58
C: Reaction time, h	1	2	3	4

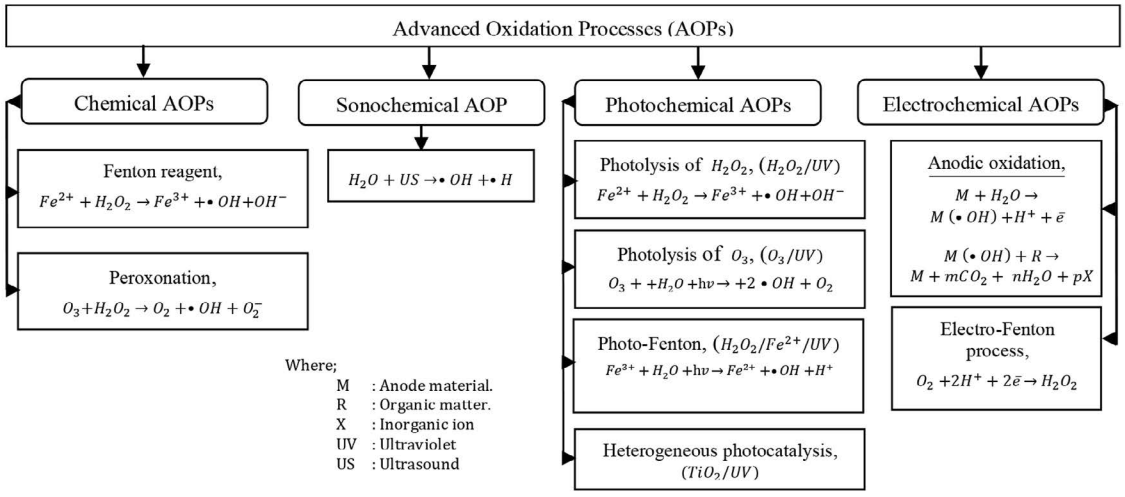

Fig. 1. Main methods accepted under advanced oxidation processes and its basic equations.

2. Materials and method

In this study on optimization of the treatability of raw dye wastewater with the Fenton process using Minitab 19. The material and method parts are planned to be given under two subheadings: (1) material and method of working matrix design; (2) material and method of laboratory studies. The removal efficiency of the pollutant was calculated using Eq. (1).

$$\%\text{Removal} = \left[\frac{C_i - C_e}{C_i}\right] \times 100 \quad (1)$$

where C_i is the initial concentration and C_e is the final concentration of the pollutant (mg/L).

2.1. Material and method of working matrix design

In this study, both the design of the experimental batch study scope in the laboratory and the statistical analysis of the results were carried out with Minitab (Minitab 19.0). One of Minitab's software tools is the Taguchi method, and the method was used to determine the extent to which independent variables affect the experimental design and the removal of dependent variables. As is known, the Taguchi method consists of experimental design processes involving orthogonal arrays (OAs). Here, OA is the number of trials or total degrees of freedom in the matrix containing the sets in which the experimental runs will be made, and it is submitted to a tentative matrix planned with the Li phase, which includes a series of experiments in which the situation of independent factors is changed. OA makes possible the efficient determination of the outcome of various factors. The numbers and levels of control factors in the experimental study directly affect the selection of an appropriate OA [26,29]. The method was used to decide on the most suitable conditions for both independent and dependent variables in this study. For this purpose, during the experimental design process, reaction time, H_2O_2 and Fe^{2+} concentrations were chosen as independent variables in batch studies. Each independent variable is planned at four levels. It was aimed to create the ideal conditions for PIWW purification by making the least number of experimental studies for each variable consisting of L_{16} orthogonal arrays. The independent variables included in the study plan and the levels of the independent variables to be used in discrete studies are presented in Table 2.

Moreover, in this study, Minitab was used to generate the regression equations and surface and counter graphs, to make analysis of variance (ANOVA) analyses, and to optimize the study parameters. Regression analysis and related figures, tables, and equations were performed using Minitab 19 software and regression model tools. The graphics were also made using the "contour plot, and surface plot" sections under the same tools. Optimum operating conditions are also obtained with the help of the "response optimizer" under the same tool. The determination of experimental conditions, working matrix design, and S/N graphics were obtained with the help of Taguchi tools.

2.2. Material and method of laboratory studies

In the study, PIWW was taken from the dye production factory in the Marmara Region of Turkey. The raw wastewater was taken as a 2-h composite from the equalization pool of the paint factory. PIWW stayed in a refrigerator at +4°C in the laboratory. PIWW was taken from the refrigerator, and experimental studies were not started until the temperature of PIWW had increased to the temperature of the environment in the laboratory. Information on the physicochemical content of PIWW is presented in Table 1. 0.5-L Plexiglas reactors were used for each batch experiment. Each experimental study was performed with 0.2 L of raw PIWW based on Tables 1 and 2. All batch studies were performed at the current pH of PIWW, so no pH adjustment was done. Measurements of conductivity and pH were done with WTW pH/conductivity 340i SET 2. COD analyses were done with the closed reflux method. Moreover, the platinum-cobalt method [30] was used to determine the color pollution of the wastewater. After each batch of work, all wastewater analyses were performed in accordance with The Standard Methods for Examination of Water and Wastewater [30]. All analyses were carried out in triplicate (each analysis was performed at least three times, and the confidence level was taken as at least 95%).

3. Results and discussion

As stated before, Minitab software was used in both the creation of the discrete experimental operating conditions and the optimization of the dependent variable removal efficiencies according to the independent variable levels. In the study, 3 independent factors and 4 levels for each independent factor were predicted (L_{16}). The purpose here is to optimize the levels of independent variables that will allow efficient removal of key pollutants associated with PIWW using the Fenton process. In order to evaluate the results of each batch, experimental trials have been created with lots of graphics (Pareto, counter, surface, etc.) based on Minitab software. In order to evaluate the effective parameters and their confidence levels on their COD and color removal efficiencies, were also used ANOVA. The purpose of the ANOVA in this study was to investigate which process parameters significantly affected process responses. Also, all variable levels in Table 2 were applied during experimental batch trials, and COD and color removal efficiencies were calculated [28] and given in Table 3.

Table 3 shows the removal efficiencies of dependent factors at the end of 16 batch experimental studies. Moreover, the ratios related to the molar masses of the independent variables used in each study set are also calculated and given in the last column of Table 3. The evaluation of the mass ratios related to the last column of Table 3 depending on the experimental study sets of the independent variables was discussed in the next section.

In Table 3, batch experiments performed in the study and pollutant removal efficiencies obtained at the end of the planned reaction times are presented. The pH value of PIWW at the beginning of each batch experiment was 5.7 (from Table 1). In the preliminary studies, it was determined that the pH value decreased in a short time due to the added

chemicals (H_2O_2 and Fe^{2+}), which are suitable for the Fenton process. Therefore, pH was not chosen as an independent factor, and the study was carried out at the current pH value of PIWW. Briefly, all Fenton process batch studies were carried out with the pH of the raw wastewater available. After the addition of Fe^{2+} and H_2O_2, the pH decreased (from Fig. 3) between 4.6 (run 9) and 3.1 (run 16) within the first 2 min. Moreover, at the end of the periods in the determined working matrix, the final pH values decreased to the range of 4.4 (run 5) and 2.7 (run 4). The treatment of wastewater without pH adjustment is considered one of the important achievements of this study. Moreover, it can be seen from Fig. 3 that in this study, without any pH adjustment, the pH range required for the Fenton process was achieved in 75% of the studies with the addition of Fenton reagents.

It can be seen from Fig. 3 that although no pH adjustment was made in the wastewater, after the Fenton reagent addition (As $FeSO_4{\cdot}7H_2O$), the pH could be maintained in the pH range required for the Fenton process (pH = 2–4) in 12 studies, except for the batch studies numbered 1, 5, 9, and 13. From Taguchi analysis, the effects of independent parameters on COD and color removal efficiencies are presented in Figs. 4 and 5, respectively.

On the left-hand side of Fig. 4, the H_2O_2 concentrations are shown (2.9, 5.8, 8.7, and 11.6 g/L). In the middle of Fig. 4, Fe^{2+} concentrations (0.14, 0.29, 0.44, and 0.58 g/L) are shown. On the right-hand side of Fig. 4, it is shown the reaction time (1, 2, 3, and 4 h) based on levels 1–4. It is seen from Fig. 4 that the H_2O_2 values at which the highest and lowest COD removal efficiencies occur are at levels 3 and 1, respectively. In addition to this, the H_2O_2 concentrations at which the highest and lowest COD removal efficiencies are obtained are 8.7 and 2.9 g/L, respectively. It is seen in Fig. 4 that the Fe^{2+} concentrations at which the highest and lowest COD

Table 3
Experimental variables, their levels, and results of conducted experiments corresponding to the L_{16} experimental plan

Runs	Variables and their levels			Removal of COD, %	Removal of Color, %	COD/H_2O_2/Fe^{2+}
	A	*B*	*C*			
1	1	1	1	55	85	1.0/0.45/0.02
2	1	2	2	58	88	1.0/0.45/0.05
3	1	3	3	61	89	1.0/0.45/0.07
4	1	4	4	52	80	1.0/0.45/0.09
5	2	1	2	57	86	1.0/0.91/0.02
6	2	2	1	57	87	1.0/0.91/0.05
7	2	3	4	55	90	1.0/0.91/0.07
8	2	4	3	64	87	1.0/0.91/0.09
9	3	1	3	69	93	1.0/1.36/0.02
10	3	2	4	69	98	1.0/1.36/0.05
11	3	3	1	56	92	1.0/1.36/0.07
12	3	4	2	65	90	1.0/1.36/0.09
13	4	1	4	66	86	1.0/1.81/0.02
14	4	2	3	59	91	1.0/1.81/0.05
15	4	3	2	63	85	1.0/1.81/0.07
16	4	4	1	58	88	1.0/1.81/0.09

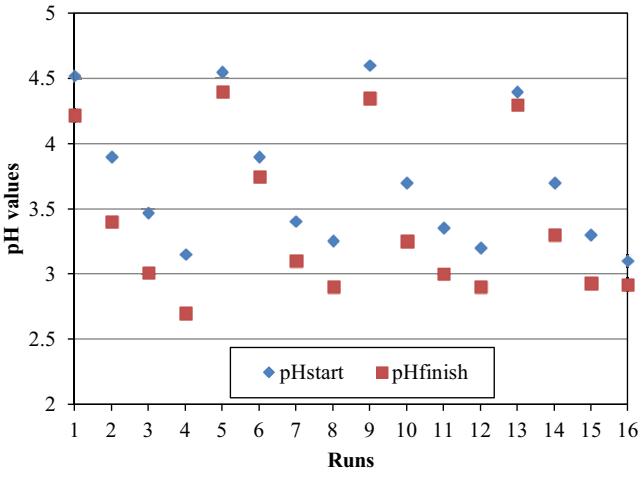

Fig. 3. pH values measured at the beginning after adding catalyst (pHstart) and at the end of the reaction time (pHfinish) of each working set in the Fenton process.

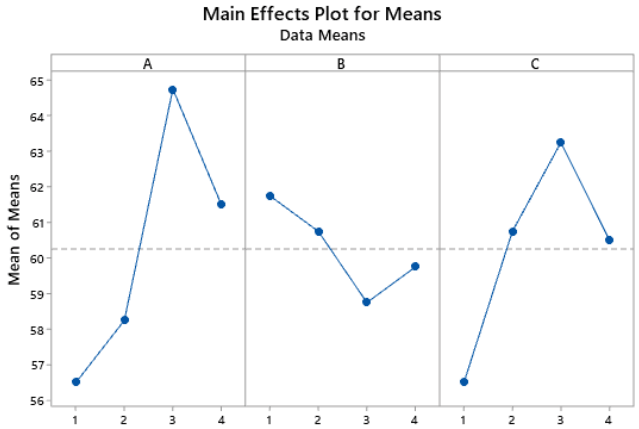

Fig. 4. Effect of each independent parameter on chemical oxygen demand removal efficiency.

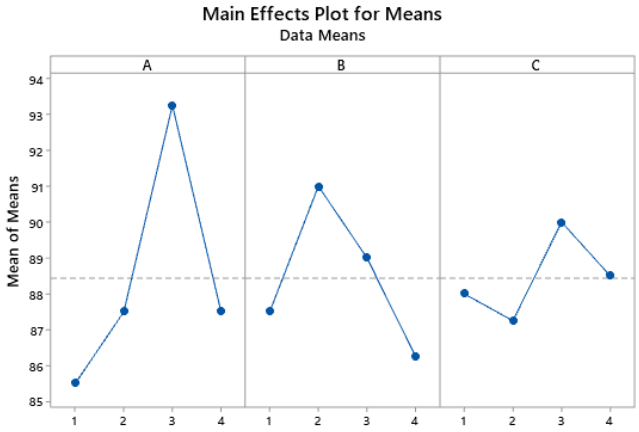

Fig. 5. Effect of each independent parameter on color removal efficiency.

removal efficiencies occur are levels 1 and 3, respectively. In addition to this, the Fe^{2+} concentrations values at which the highest and lowest COD removal efficiencies occur are 0.14 and 0.44 g/L, respectively. It is shown in Fig. 4 that the reaction times at which the highest and lowest COD removal efficiencies occur are levels 3 and 1, respectively. In addition to this, the reaction time values at which the highest and lowest COD removal efficiency occur are 3 and 1 h, respectively. According to Fig. 4, it can also be said that COD removal tends to increase with the increase of H_2O_2 concentration, but it tends to decrease with the increase of Fe^{2+} concentration.

On the left-hand side of Fig. 5, the H_2O_2 concentrations are shown. In the middle of Fig. 5, Fe^{2+} concentration values are shown. On the right-hand side of Fig. 5, reaction times are shown based on four levels. It is seen from Fig. 5 that the H_2O_2 values at which the highest and lowest color removal efficiencies occur are at levels 3 and 1, respectively. In addition to this, the H_2O_2 concentrations at which the highest and lowest color removal efficiencies are obtained are 8.7 and 2.9 g/L, respectively. It is seen in Fig. 5 that the Fe^{2+} concentrations at which the highest and lowest COD removal efficiencies occur are levels 2 and 4, respectively. In addition to this, the Fe^{2+} concentration values at which the highest and lowest color removal efficiencies occur are 0.29 and 0.58 g/L, respectively. It is seen in Fig. 5 that the reaction times at which the highest and lowest color removal efficiencies occur are levels 3 and 2, respectively. In addition to this, the reaction time values at which the highest and lowest color removal efficiencies occur are 3 and 2 h, respectively. According to Fig. 5, it can also be said that COD removal tends to increase with the increase of H_2O_2 concentration and reaction time, but it tends to decrease with the increase of Fe^{2+} concentration. Moreover, contour plot and surface plot graphics are prepared by using Minitab software for the removal of dependent parameters. Depending on the independent variables, surface and contour graphics can be used to better see the removal efficiency of the pollutant parameters. In this context, surface and contour graphs for both COD and color removal efficiencies were prepared in order to see at which independent variable levels and which levels of pollutant removal efficiency could be achieved. Related graphs of color and COD removal efficiencies are given in Figs. 6 and 7, respectively.

Fig. 6a shows the surface plot of the effect of the independent variables H_2O_2 and Fe^{2+} on the color removal efficiency, while Fig. 6b shows the contour plot. From Fig. 6a and b, it can be seen that lower removal efficiencies were obtained for color removal at relatively high concentrations of these two independent variables compared to studies with relatively low concentrations. This shows that increasing independent variable levels after a certain level has a negative effect on the color removal efficiency. However, it is seen that over 90% color removal efficiency is obtained for almost all levels of these two independent variables. In Fig. 6c and d, the effect of H_2O_2 concentration and reaction time on the color removal efficiency is seen. It is observed that at high levels of relief and at high levels of the duo, the efficiency is relatively low (>65) at the points where one is low (>90%) and at the points where both are low. Fig. 6e and f are graphs related to the effect of Fe^{2+} and the reaction time independent variable pair on color removal. As can be seen from these surface and contour graphs, it is understood that the removal efficiency is high (>90%) at points where Fe^{2+} concentration and reaction time are high. It is observed that the yield is medium-high (>80) at the points where one is low and relatively low (>60) at the points where both are low.

Fig. 7a shows the surface plot of the effect of the independent variables H_2O_2 and Fe^{2+} on the COD removal efficiency, while Fig. 7b shows the contour plot. From Fig. 7a and b, it can be seen that at high or low concentrations of both parameters, a medium level of removal (50%–55%) is obtained for COD removal, while at the points where either one is high, the maximum removal efficiency (>65%) is reached for COD. In Fig. 7c and d, the effect of Fe^{2+} and reaction time independent variables on COD removal efficiency is seen. It is seen that at low or high levels of both parameters, a medium level of removal (50%–55%) for COD removal is obtained, while at the points where either one is high, the maximum removal efficiency (>65%) is reached for COD. In Fig. 7e and f, the effect of reaction time with Fe^{2+} on the efficiency of COD removal is seen. It is seen that COD removal efficiency is moderate (>50%–55%) at points where Fe^{2+} concentration and reaction time are both high and low. It is understood that relatively higher removal efficiencies (>60) are achieved at points where one is low and the other is high.

An ANOVA was performed to examine the effective parameters and their confidence levels on the COD and color removal efficiencies. ANOVA is used to explore which process parameters significantly affect the process responses. The first parameter analyzed in the process was COD. According to the ANOVA values obtained from Table 4, F = 154.19 ($F > F_{table}$). The model equation with a 95% confidence level is given in Eq. (2).

$$\%\text{COD removal} = 3.74A + 148.8B + 19.58C - 7.71AB - 0.686AC - 41.5BC; \quad (p < 0.05) \tag{2}$$

The second parameter analyzed with the Al–Al electrode pair in the process was color. According to the ANOVA values obtained from Table 4, F = 159.13 ($F > F_{table}$). The model equation with a 95% confidence level is given in Eq. (3).

$$\%\text{Color removal} = 7.4A + 186.5B + 31.9C - 10.87AB - 1.97AC - 54.3BC; \quad (p < 0.05) \tag{3}$$

The coefficients of the equations show the degree of effect of each parameter on the removal of each pollutant. These effects can be seen more clearly from the Pareto charts, where the most important independent variable that plays a role in the removal of COD is Fe^{2+} (23.87%). Moreover, the second and third important degrees of effect on COD removal were obtained as reaction time (21.67%) and H_2O_2 (12.01%), respectively. As a result, the order of the independent variables according to their degree of effect on COD removal can be ordered from largest to smallest as Fe^{2+} concentration > reaction time > H_2O_2 concentration. The results of the Pareto chart regarding the color removal performance in the same table are also included. As stated

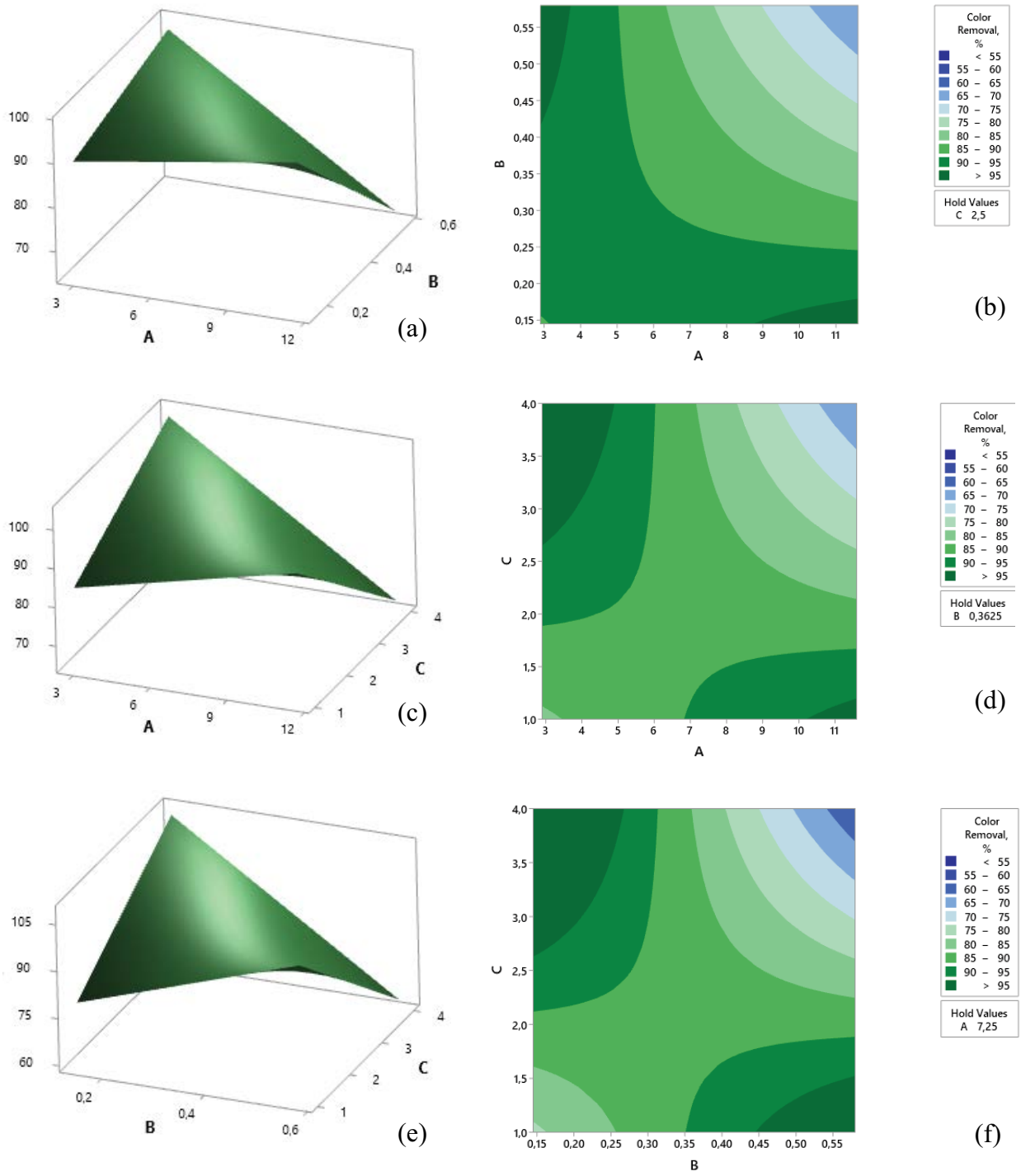

Fig. 6. Contour and surface graphics for color removal.

before, the independent variables in the tables are listed in order of importance according to the removal of the dependent variables. It is seen that the independent variable that has the greatest degree of effect on the effective removal of color is reaction time (22.42%). Moreover, the second and third degrees of effect on color removal were Fe^{2+} (19.00%) and H_2O_2 (15.08%), respectively. As a result, the order of the independent variables according to their degree of effect on color removal can be ordered from largest to smallest as reaction time > Fe^{2+} concentration > H_2O_2 concentration.

Optimum operating conditions and an estimation of the response under these conditions are shown in Table 4.

According to Table 4, the best conditions for COD removal efficiencies in the study were estimated at 8.7 g/L, 0.14 g/L, and 3 h for H_2O_2 concentration, Fe^{2+} concentration and reaction time, respectively. Under these conditions, the

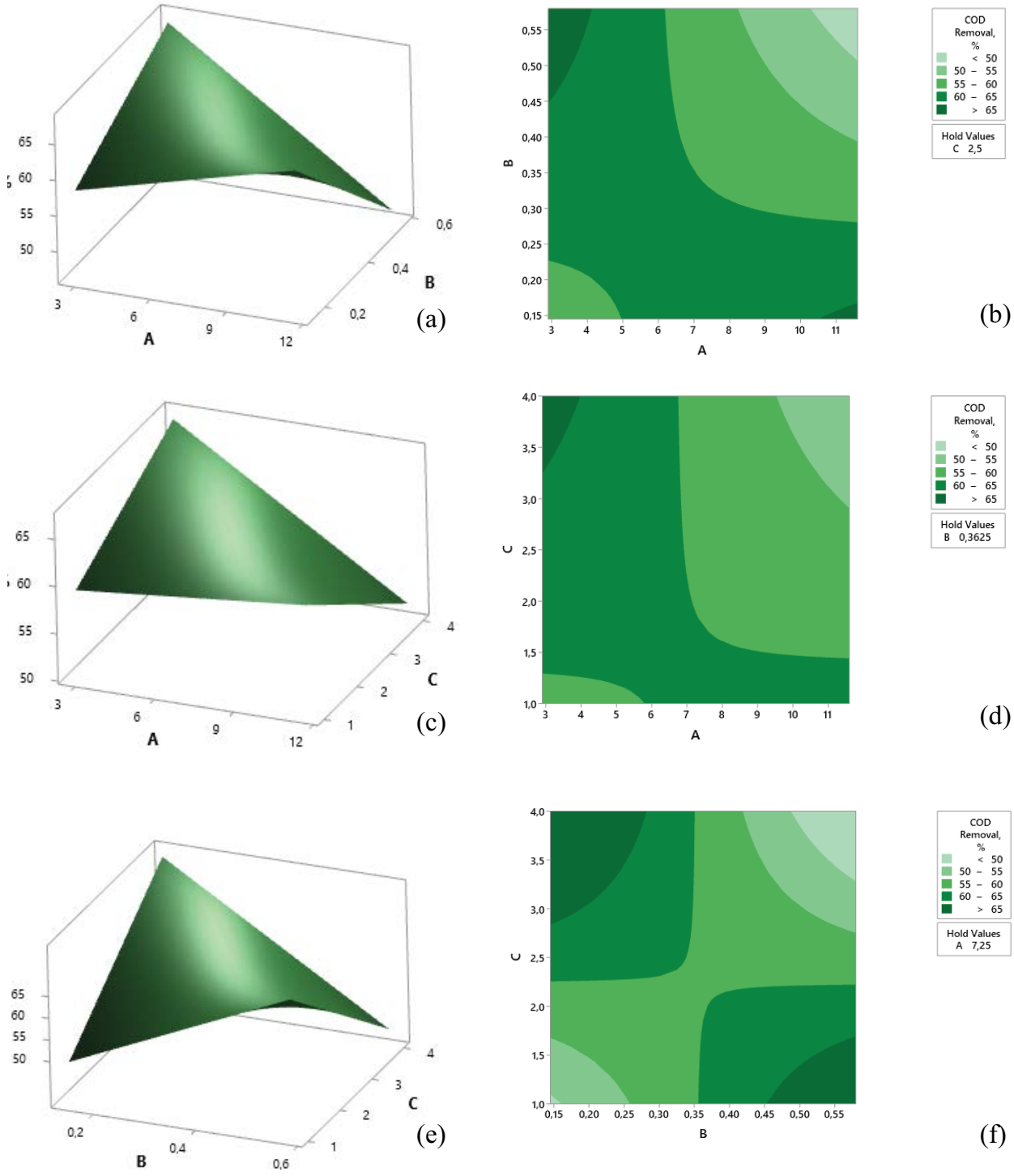

Fig. 7. Contour and surface graphics for chemical oxygen demand removal.

Table 4
Predicted pollutant removal efficiency values for optimum experimental conditions

Sources	H_2O_2	Fe^{2+}	Reaction time	Predicted, %	95% CI
Chemical oxygen demand	11.6	0.154	3.99	75.48	(57.60–97.70)
Color	11.6	0.154	3.99	>99.00	(87.11–109.9)

estimation of COD removal efficiency was calculated at 72.75%. According to Table 4, the best conditions for color removal efficiencies were estimated at 8.7 g/L, 0.29 g/L, and 4 h for H_2O_2 concentration, Fe^{2+} concentration and reaction time, respectively. Under these conditions, the estimation of color removal efficiency was calculated at 95.88%. A comparison of the model and test results separately for both COD and color removal is given in Fig. 8.

Looking at Fig. 8 and the results of the regression analysis, it is seen that there is a high correlation between the graphs of the estimation equations of COD and color removal produced based on three independent parameters and the graphs of the test results (>90%).

The symbols expressed as triangles in Fig. 8 are the color removal efficiencies and the removal efficiencies obtained as a result of the model. As you can see it is extremely close. Similarly, circular symbols indicate that COD removal prefers the experimental model. In Fig. 8 the straight lines represent the results and the dashed lines represent the results of the model [31]. It is seen that the results are in the 95% confidence interval and are highly received in writing. If these results are close to each other, the model is more successful [32]. As a matter of fact, it is seen in Fig. 8 that they are extremely close to each other [31–33].

Each batch study was done within the scope of the study matrix given in Table 3. For this reason, in many batch experiments performed in the study, the planned reaction time expires before the added H_2O_2 is consumed. Therefore, all of the H_2O_2 added to the reaction reactor cannot be consumed due to the reaction time constraint [34]. Since spent H_2O_2 is taken into account in cost calculations, unit treatment costs may be higher than expected. In conclusion, run 1 has the lowest unit treatment cost, with 14% less treatment efficiency compared to run 9, which has the highest COD removal performance. Considering all runs (study sets), unit treatment costs are higher than expected since H_2O_2 is the determining factor in unit treatment costs (6.5–30.8 USD/m^3 PIWW). In run 1, where the lowest cost was achieved, 14% less COD removal efficiency was obtained than in run 9, where the highest removal efficiency was obtained. Run 3, which has 8% less removal efficiency than run 9, where the highest removal efficiency is obtained, can be considered the optimum study set in this study. Run 3, where both the COD efficiency and the H_2O_2 dose are low, can be considered the optimum unit

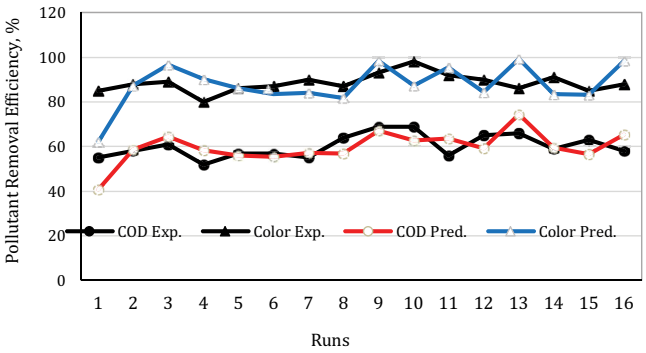

Fig. 8. Comparison of the model and batch study results separately for both chemical oxygen demand and color removal.

treatment cost set. As a result, in this study, the unit PIWW treatment cost can be accepted as 7.15 USD/m^3 PIWW.

In this study, in which the treatment of PIWW wastewater with the Fenton process was optimized, it is thought that the higher removal efficiency than the expected pollutant efficiencies with the theoretical hydrogen peroxide addition is due to the synergistic effect of the components in the Fenton process, and the situation is discussed under the title "Synergistic effect of the Fenton process on the PIWW treatment". Moreover, the effects of the independent variables on the pollutant removal efficiency are discussed separately for each of the three independent variables under the title "Effect of operating parameters on the process".

3.1. Synergistic effect of Fenton process on PIWW treatment

The Fenton process is the most popular for wastewater treatment among all available AOPs. Numerous endeavors have been devoted to improving the oxidation efficiency of the Fenton reaction in terms of promoting •OH generation, accelerating the iron redox cycle, and extending the applicable pH range. However, in addition to oxidation, coagulation and adsorption also simultaneously occur in the Fenton process, which play important roles in the removal of pollutants. Rapid progress has revealed the synergistic effects of oxidation, coagulation, and adsorption in the Fenton process, providing new ideas for the treatment of complex and refractory wastewater [35].

The synergistic effect is the effect of the hydroxyl radical, which has a much stronger oxidation potential than hydrogen peroxide. The activity of the hydroxyl radical is determined by the Fe and H_2O_2 doses and the characterization of the water. Some reactions in the environment affect the oxidation negatively and reduce the removal efficiency. When the COD/H_2O_2/Fe ratios in Table 5 are compared

Table 5
Synergistic effect of Fenton process on paint industry wastewater in terms of chemical oxygen demand removal

Runs	COD/H_2O_2/Fe^{2+}	E_{th}, %	E_{FP}, %	SEoFP, %
1	1.0/0.45/0.02	21	55	162
2	1.0/0.45/0.05	21	58	176
3	1.0/0.45/0.07	21	61	190
4	1.0/0.45/0.09	21	52	148
5	1.0/0.91/0.02	43	57	33
6	1.0/0.91/0.05	43	57	33
7	1.0/0.91/0.07	43	55	28
8	1.0/0.91/0.09	43	64	49
9	1.0/1.36/0.02	64	69	8
10	1.0/1.36/0.05	64	69	8
11	1.0/1.36/0.07	64	56	–13
12	1.0/1.36/0.09	64	65	2
13	1.0/1.81/0.02	86	66	–23
14	1.0/1.81/0.05	86	59	–31
15	1.0/1.81/0.07	86	63	–27
16	1.0/1.81/0.09	86	58	–33

with the time and removal efficiency, the results may be evaluated as a success of the Fenton reaction.

Three of the reactions of H_2O_2 in an acidic solution are presented in Eqs. (4)–(6).

$$H_2O_2 \rightarrow \frac{1}{2}O_2 + H_2O \quad (4)$$

$$CH_4 + 2O_2 \rightarrow CO_2 + 2H_2O \quad (5)$$

$$CH_4 + 4H_2O_2 \rightarrow CO_2 + 6H_2O \quad (6)$$

From Eq. (4) the theoretical H_2O_2 requirement for 1 g COD removal can be calculated as 2.125 g (H: 1 g/mol, O: 16 g/mol. H_2O_2/COD = 34 g·H_2O_2/0.5 × 32 g O = 2.125 g·H_2O_2/g·COD). Some equations are organized to calculate the synergistic effect of the Fenton process (SEoFP). The required dose of H_2O_2 for COD removal can be calculated from Eq. (4). The amount of H_2O_2 required for COD removal is 2.125 times that of COD, which corresponds to a 100% theoretical H_2O_2 amount. Using Eq. (4) the theoretical percentage of H_2O_2 used in the experimental study can be calculated. The other words, the theoretical H_2O_2 percentage can also be considered as the expected theoretical COD removal efficiency (E_t) and given in Eq. (7).

$$E_t = \frac{M_{H_2O_2}}{f_F COD_{in}} \times 100 \quad (7)$$

where f_F is 2.125 H_2O_2/g·COD from Eq. (4), $M_{H_2O_2}$ is used hydrogen peroxide mass used in each batch study (g/L), COD_{in} is the initial COD concentration of each batch study (g/L). The COD removal efficiency for the Fenton process (E_{FP}) in each batch study was calculated from Eq. (8).

$$E_{FP} = \frac{COD_{in} - COD_{ef}}{COD_{in}} \times 100 \quad (8)$$

where COD_{ef} is the final COD concentration of each batch study (g/L). Hence, the synergistic effect of the Fenton process on COD removal can be calculated by Eq. (9).

$$SEoFP = \frac{E_{FP} - E_t}{E_t} \times 100 \quad (9)$$

The synergistic effect of the Fenton process on COD removal for each batch study is given in Table 5. It can be seen from Table 5 that the COD removal efficiency was 69% with 64% of the theoretical H_2O_2 dose (runs 9 and 10). This result indicates that an additional 8% COD removal efficiency was achieved with the Fenton process. Similarly, for the 8th run (run 8), a 43% theoretical H_2O_2 and 64% COD removal efficiency were obtained. It can be said that the additional 49% COD removal in the 8th study was also due to the Fenton effect from Eq. (9). In addition, 21% theoretical H_2O_2 and 61% COD removal efficiency were achieved for the 3rd run (run 3). The additional COD removal efficiency in the 3rd study was obtained at 190%, and this was achieved by the Fenton effect. In the 3 h of studies discussed here, the amount of sludge obtained was 1 unit for the 9th study, 4 units for the 8th study, and 3 units for the 3rd study. The preferred work is the work that meets the discharge criteria, produces less sludge, consumes fewer chemicals, and is faster. Pollutant removal will be possible by applying low-dose Fenton oxidations in a few steps to increase efficiency.

The synergistic effect is the effect of the hydroxyl radical, which has a much stronger oxidation potential than hydrogen peroxide. The activity of the hydroxyl radical is determined by the Fe and H_2O_2 doses and the characterization of the water. For example, theoretical H_2O_2 demand for run 3 is 21% from Eq. (4), but COD removal efficiency is obtained as 55% experimentally, so 195% removal efficiency is obtained synergistically from Eq. (9). Some reactions in the environment affect the oxidation negatively (runs 11, 13–16 from Table 5) and reduce the removal efficiency. In Table 5, yields above 100% are the result of the synergistic effect of hydroxyl radicals formed by the Fenton reaction, and it is expected and desirable. It was obtained at low H_2O_2 doses and at the end of the determined reaction times, when almost all of the H_2O_2 doses were spent. Negative yields are due to unconsumable high H_2O_2 doses in limited reaction times and a slow reaction rate against resistant pollutant forms. Since the evaluations were made on the initial H_2O_2 doses, the removal efficiencies were calculated as low or negative levels in the sets (runs 9–16) using high H_2O_2 doses.

3.2. Effect of operating parameters on the process

A combination of H_2O_2 and a homogeneous solution of iron ions is described as Fenton's reagent, and the application of Fenton's reagent in any process is called the Fenton process. The Fenton process in wastewater treatment starts with the formation of hydroxyl radicals and continues with the decomposition or destruction of various organic pollutants by the formed radicals. The efficiency of Fenton's reagent powerfully depends on a variety of variables such as pH, H_2O_2 concentration, catalyst concentrations, and the rate of oxidation of organics by generated •OH [1,14,18]. As is well known, the Fenton process is very sensitive to the pH of the wastewater to be treated. The oxidation capacity of the Fenton process decreases at both low [36] and high [37] pH values. In wastewater treatment with the Fenton process, there is an optimum pH range for the degradation of organic pollutants, which is known as 2–4 for the conventional Fenton process. There is always a pH range in Fenton processes other than traditional Fenton processes. For example, the optimum pH range for the degradation of methylene blue by the heterogeneous Fenton system is 2–5 [38], natural gas extraction effluents by the photo-Fenton process are 3–6 [39], and azo dyes by the heterogeneous Fenton process are 3–9 [40]. In this study, it was determined by preliminary studies that the pH value of the wastewater to be treated with the addition of catalyst and hydrogen peroxide fell within the optimum range (Fig. 3) required for the Fenton process. Therefore, no pH adjustment was made, and pH was not included among the independent variables in this study. Hence, the operational parameters of the current study were selected as H_2O_2 concentrations, Fe^{2+} concentrations, and reaction time.

3.2.1. Effect of H_2O_2 concentration on the process

The effect of H_2O_2 concentration on the degradation of pollutants by Fenton processes is similar to that of Fe^{2+} concentration. Generally, even though the degradation efficiency of pollutants increases with increasing H_2O_2 concentration [41], they should not be added indefinitely. Because excess H_2O_2 addition not only increases operating costs but also increases the scavenging effect of radical OH by H_2O_2 [42], Therefore, it is necessary to search for an optimum H_2O_2 concentration at which maximum removal of pollutants can be achieved. It is a known fact that one of the most significant independent factors for efficient elimination of pollutants (COD and color) in the Fenton process is H_2O_2 for PIWW treatment. It is concluded that H_2O_2 concentration is one of the most important factors for both COD and color removal efficiencies for PIWW treatment. As can be seen from Figs. 4 and 5, it can be said that the COD and color removal efficiency tend to increase with the increase of the H_2O_2 dose. Also, the degree of effect of the factor on COD removal is lower (%12.01). Moreover, from Fig. 5 the highest color removal efficiency is obtained at level 3 of H_2O_2 concentration (8.7 g/L). Also, the degree of effect of the factor on color removal is lower (%15.08). The efficiencies of COD and color removal based on the variation in H_2O_2 concentration are shown in Table 3. The best removal efficiency of COD was obtained at the third level (8.7 g/L) in the PIWW treatment. On the other hand, the best removal efficiency of color was also obtained at the third level (8.7 g/L).

3.2.2. Effect of Fe^{2+} concentration on the process

Used as a catalyst in the Fenton process, Fe^{2+} is known to catalyze the decomposition of H_2O_2 to produce the highly oxidative radical OH that can degrade the most stubborn organic pollutants. Generally, even though the degradation efficiency of organic pollutants increases with increasing Fe^{2+} concentration [38], they should not be added indefinitely. Because excess Fe^{2+} addition not only increases operating costs and iron sludge production but also increases the scavenging effect of radical OH by Fe^{2+} [43], Therefore, it is necessary to search for an optimum Fe^{2+} concentration at which maximum removal of pollutants can be achieved.

In this study, one of the other vital independent factors to effectively remove pollutants (COD and color) in the Fenton process is Fe^{2+} concentration for PIWW treatment. It is concluded that Fe^{2+} concentration is one of the most important factors for both COD and color removal efficiencies for PIWW treatment. As can be seen from Figs. 4 and 5, the COD and color removal efficiency tend to decrease with the increase in Fe^{2+} dose. Also, Fig. 4 shows that the highest degree of effect on COD removal is from the Fe^{2+} factor (%23.87). Moreover, from Fig. 5, the highest color removal efficiency is obtained at level 2 of the Fe^{2+} concentration (0.29 g/L). Also, Fig. 5 shows that the highest second degree of effect on color removal is from the Fe^{2+} factor (%19). The removal efficiencies of COD and color based on the variation in Fe^{2+} concentration are shown in Table 3. The best removal efficiency of COD was obtained at the first level (0.14 g/L) in this study. On the other hand, the best removal efficiency of color was obtained at the second level (0.29 g/L).

3.2.3. Effect of reaction time on the process

Fenton processes may require long reaction times. The length or shortness of the reaction time depends on the pollutant concentrations. High pollutant concentrations may require long reaction times [44,45]. In the present study, batch treatability tests were carried out by the Fenton process, considering reaction times of 1–4 h for paint industry wastewater with a high pollution load. In this study, one of the other vital independent factors to effectively remove pollutants in the Fenton process is reaction time for PIWW treatment. It is concluded that reaction time is one of the most important factors for both COD and color removal efficiencies for PIWW treatment. As can be seen from Figs. 4 and 5, it can be said that the COD and color removal efficiency tend to increase with the increase in reaction time. Also, the second highest degree of effect on COD removal is from the reaction time factor (%21.67). Moreover, from Fig. 5, the highest color removal efficiency is obtained at level 3 of the reaction time (3 h). Also, the highest degree of effect on color removal is from the reaction time factor (22.42). The removal efficiencies of COD and color based on the variation of reaction time are shown in Table 3. The best removal efficiency of COD was obtained at the third level (3 h) in this study. On the other hand, the best removal efficiency of color was obtained at the fourth level (4 h).

4. Conclusion

PIWW, whose treatability study was carried out, was taken from the paint production factory equalization pool and includes wastewater from all production processes in the factory. For this reason, PIWW contains both water-based and oil-based paint production wastewater. It is clear that the PIWW, whose treatability study has been carried out here, can be treated at a level that can be given to the receiving environment by the Fenton process. So, this study aims to determine the working conditions that will reduce the burden of subsequent treatment processes by performing the process. The average concentration of the raw wastewater was measured as 6.4 kg/m^3, and the COD load in the run 9 set (from Table 3), where the highest efficiency of COD removal was obtained, was determined as 35.33 kg/d. From the results of the study, the highest removal efficiency of COD was obtained at 69% at runs 9 and 10. One of the most important aspects is the degree of influence of independent factors on the removal efficiencies of the pollutants. Hence, the factor degree of effect on the removal efficiency of COD has been obtained as reaction time > Fe^{2+} concentration > H_2O_2 concentration. Moreover, the best removal efficiency of color is achieved at 98% at run 10. Hence, run 10 is the highest removal efficiency level for both COD and color. The degree of effect of independent variables on the color removal efficiency is determined as H_2O_2 concentration > Fe^{2+} concentration > reaction time. One of the most important implications that should be emphasized in this study is the synergistic effect of the Fenton process on COD removal, and this effect was calculated to be between 8% (runs 9–10) and 190% (run 3) in the current study. One of the other important implications is the fact that the synergistic effect of the Fenton process may have negative values at high H_2O_2 doses (levels 3–4, runs 11, 13,

and 16). In addition, it is understood that the highest synergistic effects occur in all Fe^{2+} doses (levels 1–4) when the lowest H_2O_2 doses (level 1) are applied (runs 1–4). Another important aspect of this study is that it can be purified only with Fenton components under standard conditions of the Fenton process without using additional acids and bases.

Acknowledgment

Experimental studies were mainly carried out in Environmental Engineering Laboratory, Research Laboratory 3.

Symbols

C_i	—	Initial concentration of any pollutant, mg/L
C_e	—	Final concentration of any pollutant, mg/L
T	—	Reaction time, h, min or s
V	—	Cubic volume of the treated PIWW, m^3
R^2	—	Correlation coefficient
E_{th}	—	Theoretical COD removal efficiency
f_F	—	It is 2.125 H_2O_2/g COD from Eq. (1)
$M_{H_2O_2}$	—	Hydrogen peroxide mass used each batch study, g/L
COD_{in}	—	Initial COD concentration of each batch study, g/L
COD_{ef}	—	Final COD removal efficiency of each batch study, g/L

References

[1] N.K. Surya, M. Basavaraju, A. Adani, Sustainable treatment of paint industry wastewater: current techniques and challenges, J. Environ. Manage., 296 (2021) 113105, doi: 10.1016/j.jenvman.2021.113105.
[2] T.E. Aniyikaiye, T. Oluseyi, J.O. Odiyo, J.N. Edokpayi, Physico-chemical analysis of wastewater discharge from selected paint industries in Lagos, Nigeria, Int. J. Environ. Res. Public Health, 16 (2019) 1235, doi: 10.3390/ijerph16071235.
[3] M.A. Aboulhassan, S. Souabi, A. Yaacoubi, M. Baudu, Treatment of paint manufacturing wastewater by the combination of chemical and biological process, Int. J. Environ. Sci. Technol., 3 (2014) 1747–1758.
[4] S. Popli, U.D. Patel, Destruction of azo dyes by anaerobic–aerobic sequential biological treatment: a review, Int. J. Environ. Sci. Technol., 12 (2015) 405–420.
[5] D. Krithika, L. Philip, Treatment of wastewater from water-based paint industries using submerged attached growth reactor, Int. Biodeterior. Biodegrad., 107 (2016) 31–41.
[6] O. Dovletoglou, C. Philippopoulos, H. Grigoropoulou, Coagulation for treatment of paint industry wastewater, J. Environ. Sci. Health. Part A Toxic/Hazard. Subst. Environ. Eng., 37 (2002) 1361–1377.
[7] O.Y. Balik, S. Aydin, Coagulation/flocculation optimization and sludge production for pre-treatment of paint industry wastewater, Desal. Water Treat., 57 (2016) 12692–12699.
[8] I.G. Ezemagu, M.I. Ejimofor, M.C. Menkiti, Turbidimetric study for the decontamination of paint effluent (PE) using mucuna seed coagulant (MSC): statistical design and coag-flocculation modeling, Environ. Adv., 2 (2020) 100023, doi: 10.1016/j.envadv.2020.100023.
[9] B.K. Korbahti, N. Aktas, A. Tanyolaç, Optimization of electrochemical treatment of industrial paint wastewater with response surface methodology, J. Hazard. Mater., 148 (2007) 83–90.
[10] B.K. Korbahti, A. Tanyolaç, Electrochemical treatment of simulated industrial paint wastewater in a continuous tubular reactor, Chem. Eng. J., 148 (2009) 444–451.
[11] L.F. da Silva, A.D. Barbosa, H.M. de Paula, L.L. Romualdo, L.S. Andrade, Treatment of paint manufacturing wastewater by coagulation/electrochemical methods: proposals for disposal and/or reuse of treated water, Water Res., 101 (2016) 467–475.
[12] A.D. Barbosa, L.F. da Silva, H.M. de Paula, L.L. Romualdo, G. Sadoyama, L.S. Andrade, Combined use of coagulation (*M. oleifera*) and electrochemical techniques in the treatment of industrial paint wastewater for reuse and/or disposal, Water Res., 145 (2018) 153–161.
[13] I.S. de Oliveira, L.C. VianaVerona, V.L.V. Fallavena, C.M.N. Azevedo, M. Pires, Alkydic resin wastewaters treatment by Fenton and photo-Fenton processes, J. Hazard. Mater., 146 (2007) 564–568.
[14] U. Kurt, Y. Avsar, M.T. Gonullu, Treatability of water-based paint wastewater with Fenton process in different reactor types, Chemosphere, 64 (2006) 1536–1540.
[15] M.A. Quiroz, E.R. Bandala, C.A. Martínez-Huitle, Advanced Oxidation Processes (AOPs) for Removal of Pesticides From Aqueous Media, M. Stoytcheva, Ed., Pesticides - Formulations, Effects, Fate, InTechOpen, London, 2011.
[16] D.P. Zagklis, P.G. Koutsoukos, C.A. Paraskeva, A combined coagulation/flocculation and membrane filtration process for the treatment of paint industry wastewaters, Ind. Eng. Chem. Res., 51 (2012) 15456–15462.
[17] M.A. Oturan, J.J. Aaron, Advanced oxidation processes in water/wastewater treatment: principles and applications. A review, Crit. Rev. Env. Sci. Technol., 44 (2014) 2577–2641.
[18] M.H. Zhang, H. Dong, L. Zhao, D. Wang, D. Meng, A review on Fenton process for organic wastewater treatment based on optimization perspective, Sci. Total Environ., 670 (2019) 110–121.
[19] K. Thirugnanasambandham, V. Sivakumar, J.P. Maran, Response surface modelling and optimization of treatment of meat industry wastewater using electrochemical treatment method, J. Taiwan Inst. Chem. Eng., 46 (2015) 160–167.
[20] J.M. Parks, On stochastic optimization: Taguchi methods demystified; its limitations and fallacy clarified, Probab. Eng. Mech., 16 (2001) 87–101.
[21] K. Yang, E.C. Teo, F.K. Fuss, Application of Taguchi method in optimization of cervical ring cage, J. Biomech., 40 (2007) 3251–3256.
[22] M.P. Elizalde-Gonzalez, L.E. Garcia-Diaz, Application of a Taguchi L_{16} orthogonal array for optimizing the removal of Acid Orange 8 using carbon with a low specific surface area, Chem. Eng. J., 163 (2010) 55–61.
[23] N. Yusoff, M. Ramasany, S. Yusup, Taguchi's parametric design approach for the selection of optimization variables in a refrigerated gas plant, Chem. Eng. Res. Des., 89 (2011) 665–675.
[24] A. Deghles, U. Kurt, Treatment of raw tannery wastewater by electrocoagulation technique: optimization of effective parameters using Taguchi method, Desal. Water Treat., 57 (2016) 14798–14809.
[25] H.Y. Yen, C.P. Lin, Adsorption of Cd(II) from wastewater using spent coffee grounds by Taguchi optimization, Desal. Water Treat., 57 (2016) 11154–11161.
[26] F. Özyonar, Optimization of operational parameters of electrocoagulation process for real textile wastewater treatment using Taguchi experimental design method, Desal. Water Treat., 57 (2016) 2389–2399.
[27] F. Özyonar, H. Muratcobanoglu, O. Gökkus, Taguchi approach for color removal using electrocoagulation with different electrode connection types, Fresenius Environ. Bull., 26 (2017) 7600–7607.
[28] Ö. Apaydin, E. Özkan, Landfill leachate treatment with electrocoagulation: optimization by using Taguchi method, Desal. Water Treat., 173 (2020) 65–76.
[29] O. Gökkus, Y.S. Yildiz, B. Yavuz, Optimization of chemical coagulation of real textile wastewater using Taguchi experimental design method, Desal. Water Treat., 49 (2012) 263–271.
[30] APHA, AWWA, Standard Methods for the Examination of Water and Wastewater, 20th ed., American Public Health Association, Washington D.C., 1998.

[31] S.K. Singh, H.S. Mali, D.R. Unune, S. Wojciechowski, D. Wilczyński, Application of generalized regression neural network and Gaussian process regression for modelling hybrid micro-electric discharge machining: a comparative study, Processes, 10 (2022) 755, doi: 10.3390/pr10040755.
[32] Z. Wang, X. Jiang, B. Song, G. Yang, W. Liu, T. Liu, Z. Ni, R. Zhang, PSO-BP-based morphology prediction method for DED remanufactured deposited layers, Sustainability, 15 (2023) 6437, doi: 10.3390/su15086437.
[33] S.S. Yang, S.Y. Derakhshan, F.Y. Kong, Theoretical, numerical and experimental prediction of pump as turbine performance, Renewable Energy, 48 (2012) 507–513.
[34] J. Zhang, S. Chen, Y. Zhang, X. Quan, H. Zhao, Y. Zhang, Reduction of acute toxicity and genotoxicity of dye effluent using Fenton-coagulation process, J. Hazard. Mater., 274 (2014) 198–204.
[35] R. Lin, Y. Li, T. Yong, W. Cao, J. Wu, Y. Shen, Synergistic effects of oxidation, coagulation and adsorption in the integrated Fenton-based process for wastewater treatment: a review, J. Environ. Manage., 306 (2022) 114460, doi: 10.1016/j.jenvman.2022.114460.
[36] L.M. Nieto, G. Hodaifa, S. Rodríguez, J.A. Giménez, J. Ochando, Degradation of organic matter in olive-oil mill wastewater through homogeneous Fenton-like reaction, Chem. Eng. J., 173 (2011) 503–510.
[37] X.Q. Fan, H.Y. Hao, Y.C. Wang, F. Chen, J.L. Zhang, Fenton-like degradation of nalidixic acid with Fe^{3+}/H_2O_2, Environ. Sci. Pollut. Res., 20 (2013) 3649–3656.
[38] Q. Wang, S.L. Tian, P. Ning, Ferrocene-catalyzed heterogeneous Fenton-like degradation of methylene blue: influence of initial solution pH, Ind. Eng. Chem. Res., 53 (2014) 6334–6340.
[39] J. Zhai, H. Ma, J. Liao, M.H. Rahaman, Z. Yang, Z. Chen, Comparison of Fenton, ultraviolet-Fenton and ultrasonic-Fenton processes on organics and colour removal from pre-treated natural gas produced water, Int. J. Environ. Sci. Technol., 15 (2018) 2411–2422.
[40] Z.X. Liu, L.J. Zhang, F.H. Dong, J. Dang, K.L. Wang, D. Wu, J. Zhang, J. Fang, Preparation of ultrasmall goethite nanorods and their application as heterogeneous Fenton reaction catalysts in the degradation of azo dyes, ACS Appl. Nano Mater., 1 (2018) 4170–4178.
[41] X.H. Li, S. Chen, I. Angelidaki, Y.F. Zhang, Bio-electro-Fenton processes for wastewater treatment: advances and prospects, Chem. Eng. J., 354 (2018) 492–506.
[42] C.J. Hu, D.L. Huang, G.M. Zeng, M. Cheng, X.M. Gong, R.Z. Wang, W.J. Xue, Z.X. Hu, Y.N. Liu, The combination of Fenton process and *Phanerochaete chrysosporium* for the removal of bisphenol A in river sediments: mechanism related to extracellular enzyme, organic acid and iron, Chem. Eng. J., 338 (2018) 432–439.
[43] M. Panizza, G. Cerisola, Electro-Fenton degradation of synthetic dyes, Water Res., 43 (2009) 339–344.
[44] S.G. Poulopoulos, M. Nikolaki, D. Karampetsos, C.J. Philippopoulos, Photochemical treatment of 2-chlorophenol aqueous solutions using ultraviolet radiation, hydrogen peroxide and photo-Fenton reaction, J. Hazard. Mater., 153 (2008) 582–587.
[45] O.G. Rodríguez, J.A. Bañuelos, A. El-Ghenymy, L.A. Godínez, E. Brillas, F.J. Rodríguez-Valadez, Use of a carbon felt-iron oxide air-diffusion cathode for the mineralization of Malachite Green dye by heterogeneous electro-Fenton and UVA photoelectro-Fenton processes, J. Electroanal. Chem., 767 (2016) 40–48.